Pulsed-field ionization threshold photoelectron spectroscopy with coherent extreme ultraviolet radiation: A comparison of CO and N2

W. Kong, D. Rodgers, J. W. Hepburn, Kwanghsi Wang, and V. McKoy

Citation: The Journal of Chemical Physics **99**, 3159 (1993); doi: 10.1063/1.465176
View online: http://dx.doi.org/10.1063/1.465176
View Table of Contents: http://scitation.aip.org/content/aip/journal/jcp/99/5?ver=pdfcov
Published by the AIP Publishing

Pulsed-field ionization threshold photoelectron spectroscopy with coherent extreme ultraviolet radiation: A comparison of CO and N_2

W. Kong, D. Rodgers, and J. W. Hepburn
Center for Molecular Beams and Laser Chemistry, University of Waterloo, Waterloo, Ontario N2L 3G1, Canada

Kwanghsi Wang and V. McKoy
Arthur Amos Noyes Laboratory of Chemical Physics,[a] California Institute of Technology, Pasadena, California 91125

(Received 10 March 1993; accepted 10 May 1993)

Single-photon zero-kinetic-energy pulsed-field-ionization spectra have been measured for the $v^+=0$ and 1 levels of CO^+ ($X\,^2\Sigma^+$) and the $v^+=0$ level of N_2^+ ($X\,^2\Sigma_g^+$) by coherent XUV radiation. In spite of similarities in the electronic structure of CO and N_2, the measured ion spectra show dramatically different intensities for the Q branches. These threshold spectra are interpreted on the basis of *ab initio* calculations of the ion rotational distributions. Agreement between the calculated and measured spectra is very encouraging. Improved values for the ionization potentials of CO (113 025.6 and 115 211.2±1.5 cm^{-1} for $v^+=0$ and 1, respectively) are reported and the unusual dynamics favoring $\Delta N<0$ transitions are discussed. The CO spectra show quite different behavior for the $\Delta N<0$ transitions for $v^+=0$ and $v^+=1$ bands, which is interpreted in terms of the relative importance of rotational autoionization in the two bands.

I. INTRODUCTION

With the recent development of zero-kinetic-energy (ZEKE) photoelectron spectroscopy, based on the detection of photoelectrons produced by delayed pulsed-field ionization (PFI) of very high Rydberg levels, it is now possible to exploit the narrow bandwidth of laser radiation to achieve sub-wave-number resolution in ion rovibronic state distributions.[1–3] The unprecedented resolution of this technique has led to a surge of experimental[1–8] and theoretical[7–11] activity aimed at understanding the highly state-resolved molecular photoelectron spectra which this technique provides. Recently, Pratt[12] and Chupka[13] have presented detailed and insightful analyses of the technique including the unexpectedly long lifetimes of the very high lying Rydberg states that are pulsed field ionized and the role of different processes that contribute to the observed photoelectron signal.

Originally exploited with resonance enhanced multiphoton ionization (REMPI), the technique has been extended to single-photon ionization of the ground electronic states (O_2, OH, HCl, N_2, H_2, N_2O, H_2O, and H_2S) of jet-cooled molecules by coherent vacuum ultraviolet (VUV) radiation.[7,8,11,14–19] In this paper, we report PFI-ZEKE photoelectron spectra for single-photon ionization of rotationally cold N_2 and CO molecules by *coherent extreme ultraviolet (XUV) radiation*. In spite of their similarities in electronic structure, the ion rotational distributions for these two systems can be expected to show some interesting differences due to the heteronuclear character of CO and the resulting richer angular momentum composition of its photoionization matrix elements.

In CO, both $v^+=0$ and $v^+=1$ levels of CO^+ were studied, while in N_2, only the $v^+=0$ level of N_2^+ was studied. These threshold spectra are interpreted on the basis of *ab initio* calculations of the near-threshold ion rotational distributions. The agreement between calculated and measured spectra is very encouraging. Differences seen in the calculated and measured ion rotational distributions for larger negative angular momentum changes ($\Delta N<0$) in these photoelectron spectra suggest that these peaks are enhanced by rotational autoionization.[5,8,15,16]

II. EXPERIMENTAL DETAILS

The apparatus used for these experiments has been described elsewhere[20,21] and only a brief description will be given here. Our coherent light source for single-photon ionization of CO and N_2 was based on four-wave sum-frequency mixing in pulsed jets of Kr or Xe. The laser system used to generate the coherent XUV was a pulsed dye laser system, with two dye lasers being pumped simultaneously by one Nd:YAG laser. The four-wave mixing process was resonantly enhanced with one of the dye lasers (ν_1) fixed at 2496 Å, corresponding to a two-photon transition in Xe, or 2126 Å, corresponding to a two-photon resonance in Kr, while the other laser (ν_2) was tuned to the required wavelength. By focusing the two overlapped beams into a pulsed jet, XUV at the sum frequency ($\nu_{xuv}=2\nu_1+\nu_2$) was generated. This XUV was separated from the fundamental and refocused by a normal incidence monochromator and intersected with a collimated pulsed supersonic beam. The intersection of the XUV and molecular beams defined an ionization volume which was located between the gold-mesh extraction grids of a double time-of-flight spectrometer.

For the experiments described here, a 0.25 to 2.5 V pulse was applied to one of the extraction grids 1 μs after

[a]Contribution No. 8747.

the XUV pulse, resulting in an ionizing field of 0.2–1.6 V/cm. The field-ionized electrons were swept into the flight tube by the same pulsed field and detected by a channel plate multiplier 25 cm from the ionization volume. By time gating the detection electronics on the field-ionized electron peak, it was possible to discriminate against all of the "prompt" photoelectrons. The pulsed-field-ionization–zero-kinetic-energy photoelectron (PFI-ZEKE) spectra were recorded by measuring the field ionization signal as a function of XUV wavelength and normalizing for the measured XUV intensity, which did not vary significantly over the wavelength range used in this study.

The visible laser wavelengths were calibrated using optogalvanic spectroscopy or iodine vapor laser-induced fluorescence. The absolute accuracy of the XUV photon energy was estimated to be ± 1.5 cm^{-1}. This uncertainty comes from the combined uncertainty for the two dye lasers, which are calibrated in a separate run from the PFI-ZEKE experiment. With more careful laser calibration using a monitor etalon along with simultaneous optogalvanic calibration, both being done at the same time as the PFI-ZEKE spectrum, this uncertainty could be reduced. The bandwidth of the XUV was measured by looking at sharp autoionizing resonances in Kr and was 1 cm^{-1} for the spectra reported in this paper. To calibrate the shift in ionization potential due to the ionizing field, we measured the positions of the PFI-ZEKE thresholds as a function of the pulsed field and extrapolated to zero field. Because of the intense signals observed for the $v^+=0$ bands of both N_2^+ and CO^+, we recorded these spectra under varying conditions to check for saturation of the channel plate electron detector. Some saturation was observed for conditions where the signal was maximized, but care was taken to record spectra at greatly reduced signal strength. For all of the spectra reported here, the intensities for the rotational lines were independent of XUV power.

The molecular beams used were expansions of pure N_2 or CO from a pulsed source with a nozzle diameter of 0.5 mm. Source pressures used were typically 1–2 atm. The supersonic beam was collimated by a 0.5 mm skimmer and crossed by the XUV beam about 10 cm from the nozzle. Under these conditions, we estimate the rotational temperature to be about 8 K based on REMPI experiments on NO under similar conditions,[22] analysis of the rotational structure for Rydberg resonances observed in the total ionization cross section of N_2, and the present theoretical analysis.

III. THEORY AND NUMERICAL DETAILS

A. Theory

The general theory of molecular photoionization processes used in the present studies has been described previously.[23,24] Here we present just a very brief outline of some essential features of our procedure as it is used to obtain the rotationally resolved photoelectron distributions of interest here. Under collision-free conditions, ionization originating from each of the $(2J_0+1)$ magnetic sublevels of the initial state forms an independent channel. Therefore, the total cross section σ for ionization of a J level of the initial state leading to a J^+ level of the ion can be written as[24]

$$\sigma \propto \sum_{\substack{lm \\ M_J, M_{J^+}}} \rho_{M_J M_J} |C_{lm}(M_J M_{J^+})|^2, \tag{1}$$

where $\rho_{M_J M_J}$ is the population of a specific M_J level of the initial state. The coefficients $C_{lm}(M_J M_{J^+})$ of Eq. (1) are related to the probability for photoionization of the M_J level of the initial state leading to the M_{J^+} level of the ionic state. An expression for $C_{lm}(M_J M_{J^+})$ which explicitly considers the spin coupling associated with multiplet-specific final-state wave functions and a Hund's case (b) coupling scheme for the initial and ionic states has been given by Wang and McKoy.[24] For the branching ratios of interest here, the constant implied in Eq. (1) is unimportant and will be suppressed.

A central quantity in these studies is the matrix element for photoejection of an electron from a bound molecular orbital ϕ_i into a photoelectron continuum orbital $\Psi_{f,\mathbf{k}}^{(-)}(\mathbf{r})$. Here $\mathbf{k}$ is the momentum of the photoelectron and $(-)$ denotes incoming-wave boundary conditions. The partial wave components $\psi_{klm}^{(-)}$ of $\Psi_{f,\mathbf{k}}^{(-)}(\mathbf{r})$ are defined by an expansion in spherical harmonics about $\hat{\mathbf{k}}$ of the photoelectron

$$\Psi_{f,\mathbf{k}}^{(-)}(\mathbf{r}) = \left(\frac{2}{\pi}\right)^{1/2} \sum_{lm} i^l \psi_{klm}^{(-)}(\mathbf{r})\, Y_{lm}^*(\hat{\mathbf{k}}). \tag{2}$$

Single-center expansions of $\psi_{klm}^{(-)}(\mathbf{r})$ and $\phi_i(\mathbf{r}')$, e.g.,

$$\psi_{klm}^{(-)} = \sum_{l'\lambda} g_{lm,l'\lambda}(k,r)\, \mathscr{D}_{m\lambda}^{l'} Y_{l'\lambda}(\hat{\mathbf{r}}'), \tag{3}$$

define partial wave photoelectron matrix elements $r_{fi}^{l\lambda\mu}$ in the molecular frame for ionization out of orbital $\phi_i(\mathbf{r}')$, i.e.,

$$r_{fi}^{l\lambda\mu} = \sum_{l',l_0} \langle g_{lm,l'\lambda}(k,r)\, Y_{l'\lambda}(\hat{\mathbf{r}}') \,|\, r Y_{1\mu}(\hat{\mathbf{r}}') \,|\, \phi_{il_0}(r)\, Y_{l_0,\lambda_0}(\hat{\mathbf{r}}') \rangle, \tag{4}$$

where μ is the photon polarization index in the molecular frame, m and λ are the projections of l in the laboratory and molecular frames, respectively, and $\mathscr{D}_{m\lambda}^{l}$ is a rotational matrix in Edmonds' notation.[25] Equation (4) reveals an important underlying dynamical aspect of molecular photoelectron wave functions. Whereas only $l=l'$ terms are allowed in Eq. (4) for the central fields of atomic systems, where the angular momentum of the photoelectron must be conserved, $l \neq l'$ terms arise in Eq. (4) due to the nonspherical potential fields of molecular ions. This angular momentum coupling between partial waves l and l' is brought about by the torques associated with the molecular ion potential and makes a molecular photoelectron orbital an admixture of angular momentum components. These angular-momentum changing collisions between the photoelectron and molecular ion play a crucial role in rotationally resolved molecular photoelectron spectra. The use

of molecular photoelectron orbitals which correctly incorporate such angular momentum coupling is essential at the low photoelectron energies of interest here.

B. Numerical details

The ground state wave functions of CO and N_2 used here are obtained at the self-consistent-field (SCF) level. For CO, we used a basis of (*9s5p/5s3p*) contracted Cartesian Gaussian functions of Dunning[26] augmented with one *s*, one *p*, and two *d* polarization functions centered on the nuclei (with exponents 0.075, 0.055, 0.95, and 0.25, respectively, on carbon, and 0.085, 0.065, 0.95, and 0.25, respectively, on oxygen). The total SCF energy in this basis was $-112.777\,839$ a.u. at the equilibrium internuclear distance of $R_e=2.1322a_0$.[26] The single-center expansion of the 5σ orbital around the center of mass gives 45.45% *s*, 24.12% *p*, 25.23% *d*, 2.69% *f*, 1.26% *g* ($l_0=4$), and 0.68% *h* ($l_0=5$) character at R_e. The angular momentum composition of the 5σ orbital evolves gradually from a predominant 3*s* and 3*p* admixture at smaller internuclear distance to a dominant 3*s* and 3*d* character at larger *R*. For example, the 5σ orbital has 41.51% *s*, 47.18% *p*, 8.69% *d*, 1.89% *f*, 0.22% *g* ($l_0=4$), and 0.32% *h* ($l_0=5$) character at $R=1.5a_0$ and 40.78% *s*, 5.98% *p*, 42.59% *d*, 3.05% *f*, 5.72% *g* ($l_0=4$), and 0.81% *h* ($l_0=5$) character at $R=3.0a_0$. The vibrational wave functions for the $X\,^1\Sigma^+$ ground state of CO and the $X\,^2\Sigma^+$ ground state of CO^+ were obtained by numerical integration over a range of $1.0\leqslant R\leqslant 5.0a_0$. We used the Rydberg–Klein–Rees (RKR) potential curves of Tobias *et al.*[27] for CO and those of Singh and Rai[28] for CO^+. The photoelectron matrix elements for each vibrational transition are further averaged over 12 internuclear distances between 1.5 and $3.5a_0$.

For the SCF wave functions of N_2, we used a basis of (*9s5p/4s3p*) contracted Cartesian Gaussian functions of Dunning[26] augmented with one *s* ($\alpha=0.08$), one *p* ($\alpha=0.075$), and two *d* ($\alpha=1.4836$ and 0.4691) polarization functions centered on the nitrogen atom, and two *s*, two *p*, and two *d* functions at the center of mass with exponents 0.12 and 0.045 for the *s* and *p* functions, and 0.12 and 0.025 for the *d* functions. The total SCF energy in this basis was $-108.975\,916$ a.u. at the equilibrium internuclear distance of $R_e=2.0743a_0$.[29] The single-center expansion of the $3\sigma_g$ orbital around the center of mass has 55.53% *s*, 41.01% *d*, 3.09% *g* ($l_0=4$), and 0.28% *i* ($l_0=6$) character at R_e. The $3\sigma_g$ orbital changes slowly from a predominant 3*s* character at smaller *R* (e.g., 66.33% *s* and 32.06% *d* at $R=1.6a_0$) to an equal admixture of *s* and *d* waves at larger *R* (e.g., 43.26% *s* and 47.24% *d* at $R=3.0a_0$).

For the final state, we assume a frozen-core Hartree–Fock model in which the core orbitals are taken to be those of the ion and the photoelectron orbital is obtained as a solution of a one-electron Schrödinger equation containing the Hartree–Fock potential of the molecular ion $V_{\text{ion}}(\mathbf{r},R)$, i.e.,

$$\left[-\frac{1}{2}\nabla^2+V_{\text{ion}}(\mathbf{r})-\frac{k^2}{2}\right]\psi_{klm}^{(-)}=0, \tag{5}$$

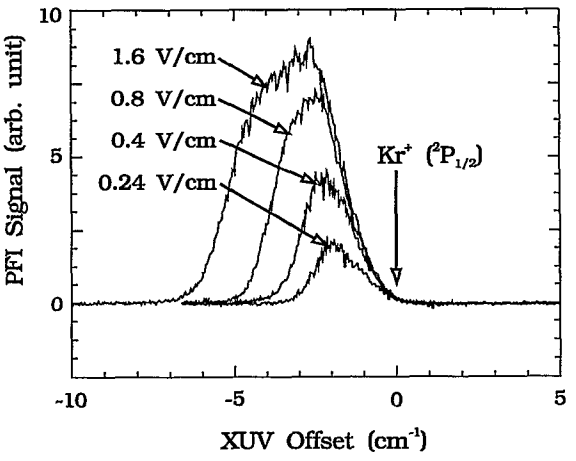

FIG. 1. The PFI-ZEKE spectrum of Kr around the Kr^+ ($^2P_{1/2}$) limit for different ionizing fields. The limit marked on the figure is the result of the extrapolation to zero field shown in Fig. 2.

where $k^2/2$ is the kinetic energy of the photoelectron. To obtain the partial wave photoelectron orbitals $\psi_{klm}^{(-)}$, we use an iterative procedure, based on the Schwinger variational principle, to solve the Lippmann–Schwinger equation associated with Eq. (5).[30] Three iterations provided highly converged solutions for the molecular photoelectron orbitals used here. Further details of calculations can be found in Refs. 30 and 31.

IV. RESULTS AND DISCUSSION

These experiments provide a direct measurement of the ionization potential of CO. To do this accurately, we measured the PFI-ZEKE spectrum of CO in the region of the lowest ionization threshold and also calibrated the apparatus through a study of Kr ionization. The line shape for the PFI-ZEKE spectrum around the $Kr^+(^2P_{1/2})$ threshold as a function of pulsed-field strength is shown in Fig. 1. A plot of the shifted ionization threshold as a function of the square root of the ionizing field is given in Fig. 2. The resulting extrapolated zero-field-ionization potential

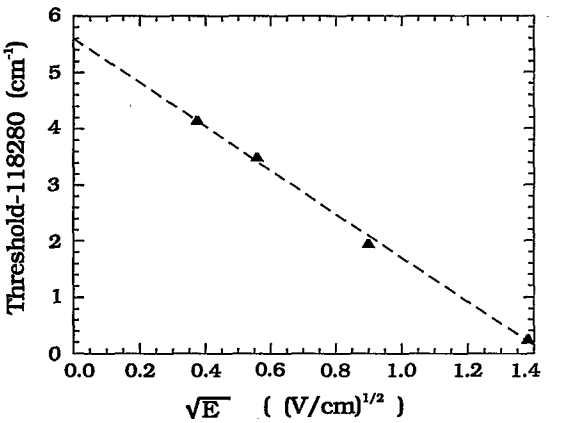

FIG. 2. The PFI threshold for Kr plotted as a function of the square root of the ionizing field. The line is the fit to the data.

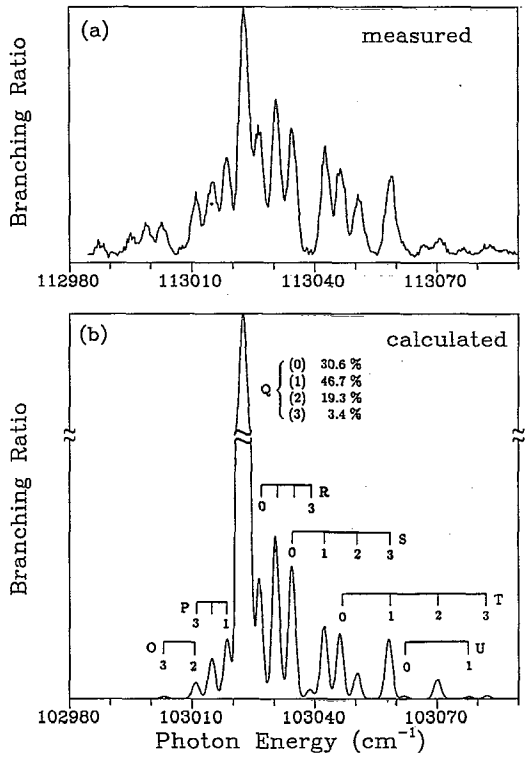

FIG. 3. (a) Measured and (b) calculated PFI-ZEKE photoelectron spectra for single-photon ionization of rotationally cold CO ($X\,^1\Sigma^+$, $v''=0$) by coherent XUV radiation leading to CO^+ ($X\,^2\Sigma^+$, $v^+=0$). The calculated spectrum assumes a temperature of 8 K and is convoluted with a Gaussian detection function with an FWHM of 2 cm^{-1}.

is the same as the literature value within experimental accuracy.[32] The line shapes for isolated rotational lines of CO and N_2 were identical to those for Kr recorded at the same ionizing field, and thus the same extrapolation could be used for the PFI-ZEKE spectra of CO and N_2. The lack of PFI signal at the actual field-free ionization threshold is caused by small stray fields in the ionization region, estimated to be on the order of 20 mV/cm.

The measured PFI-ZEKE spectrum for CO^+ ($v^+=0$) is shown in Fig. 3(a). This spectrum was recorded using a 0.4 V/cm pulsed-ionization field with a 1 μs delay after the XUV pulse. Under these conditions, there is a shift of $\sim$2.8 cm^{-1} for the measured PFI-ZEKE peak centers and the zero-field thresholds. Taking this into account, the measured CO^+ [$X\,^2\Sigma^+$ ($v^+=0$, $J^+=1/2$, $N^+=0$)]$\leftarrow$CO [$X\,^1\Sigma^+$ ($v''=0$, $J''=N''=0$)] transition energy is 113 025.6$\pm$1.5 cm^{-1}. This value is in excellent agreement with a recently obtained value of 113 027$\pm$2 cm^{-1} by extrapolation of Rydberg series.[33] Because of rotational cooling, only transitions from $N''=0$, 1, and 2 have significant intensity. The relative intensities of the rotational lines were found to be extremely reproducible and did not vary with ionizing field strength or time delay for the ionizing pulse.

Figure 3(b) shows the calculated PFI-ZEKE photoelectron spectrum for single-photon ionization of rotationally cold CO ($X\,^1\Sigma^+$, $v''=0$) molecules. The calculated ion rotational distribution assumes a temperature of 8 K. This spectrum was calculated for a photoelectron energy of 50 meV and convoluted with a Gaussian detection function with a full-width at half-maximum (FWHM) of 2 cm^{-1}. The letter designation on each branch refers only to the change of angular momentum apart from spin ($\Delta N=N^+-N''$). The agreement between these calculated and measured rotational branching ratios is very encouraging except for the Q ($\Delta N=0$) branches. Although the Q ($N''=0$–3) branches are the strongest in both spectra, the calculated spectral intensity is about ten times larger than that of the $R(1)$ transition. This behavior is indicated by the broken scale in Fig. 3(b). These intense Q branches arise from the dominant $l=1$ partial wave contribution to the photoelectron matrix element reflecting the 45% s and 25% d character of the 5σ orbital and the parity selection rule of $\Delta N+l=$odd.[23,24,34,35] Another factor which also enhances the Q branches significantly is that these branches are much denser than the spectral resolution due to the small difference in rotational constants between the ground states of CO and CO^+. Note that the same photoelectron matrix elements are used in the calculation of the spectral intensities of the Q and other branches. The origin of this disagreement between the measured and calculated spectra is not yet clear. Peaks corresponding to the $N(4)$, $O(4)$, and $N(3)$ transitions are seen in the low energy side of the measured spectrum. The calculated spectrum shows no positive or negative ΔN peaks for transitions out of the $N''=4$ level due to the vanishingly small population in this level at the temperature of 8 K assumed here. The presence of $N(4)$ and $O(4)$ peaks in the measured spectrum shows that, in fact, this $N''=4$ level has a nonvanishing population under the actual conditions of the experiment.

The calculated spectral intensity of the $O(2)$ ($\Delta N=-2$) branch is about half that of the $S(2)$ ($\Delta N=2$) branch, while these branches have almost the same intensities in the measured spectra of Fig. 3(a). Similar behavior favoring *negative* ΔN transitions is also seen in the $N(4)$, $O(4)$, $N(3)$, and $O(3)$ branches in the measured spectrum. Such enhancement of negative ΔN branches over their positive counterparts has also been seen in the threshold photoionization spectra of N_2O (Ref. 15), OH (Ref. 8), and HCl (Refs. 15 and 16) and in the threshold photoelectron spectra for (1+1′) REMPI of NO via the $A\,^2\Sigma^+(3s\sigma)$ Rydberg state.[6,36,37] A field-induced autoionization mechanism involving the interaction of high-n Rydberg states ($n>150$) with lower-n levels ($20<n<80$) converging to higher rotational thresholds of the cation has successfully accounted for this behavior.[15]

Figure 4(a) shows the measured and Fig. 4(b) shows the calculated PFI-ZEKE spectra for single-photon ionization of rotationally cold CO ($X\,^1\Sigma^+$, $v''=0$) molecules by coherent XUV radiation leading to the $v^+=1$ level of CO^+ ($X\,^2\Sigma^+$). One major difference between the spectra shown is that the overall intensity for the $v^+=1$ band is about 30 times lower than the $v^+=0$ band at the same XUV power. These calculated and measured spectral profiles are generally similar to those for CO^+ ($v^+=0$) of Fig. 3. This behavior is entirely expected for these low vibrational lev-

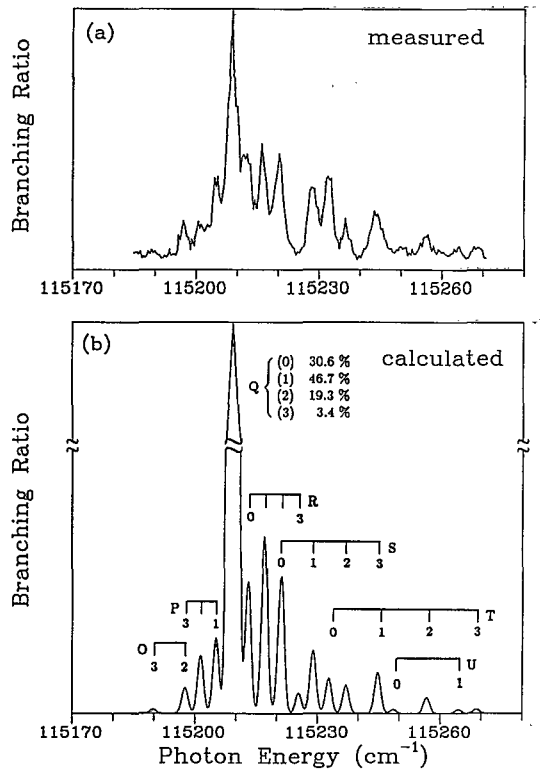

FIG. 4. (a) Measured and (b) calculated PFI-ZEKE photoelectron spectra for single-photon ionization of rotationally cold CO ($X\,^1\Sigma^+$, $v''=0$) by coherent XUV radiation leading to CO^+ ($X\,^2\Sigma^+$, $v^+=1$). The calculated spectrum assumes a temperature of 8 K and is convoluted with a Gaussian detection function with an FWHM of 2 cm^{-1}.

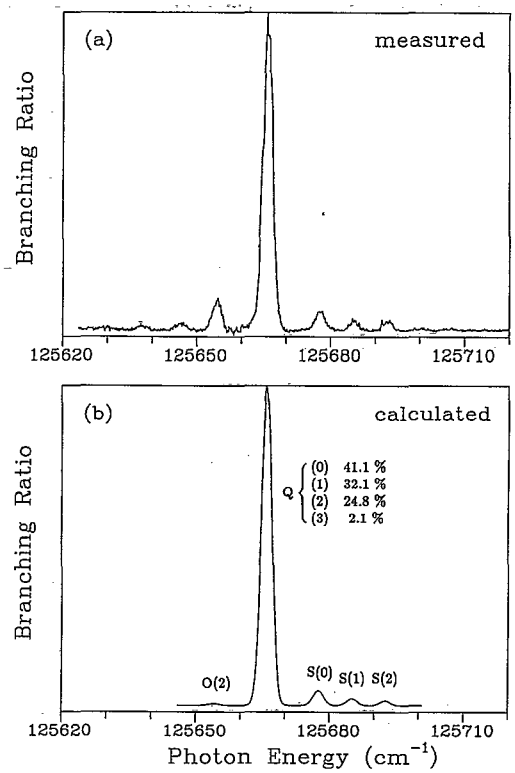

FIG. 5. (a) Measured and (b) calculated PFI-ZEKE photoelectron spectra for single-photon ionization of rotationally cold N_2 ($X\,^1\Sigma_g^+$, $v''=0$) by coherent XUV radiation leading to N_2^+ ($X\,^2\Sigma_g^+$, $v^+=0$). The calculated spectrum assumes a temperature of 8 K and is convoluted with a Gaussian detection function with an FWHM of 2.7 cm^{-1}.

els where the photoelectron matrix element does not depend on internuclear distance. However, these rotational distributions should depend on a vibrational level for higher levels due to the evolution of the 5σ orbital from a predominant $3s$ and $3p$ character at smaller R to a dominant $3s$ and $3d$ admixture at larger R and the subsequent dependence of the photoionization matrix element on R. In spite of the similarities between the spectra of Figs. 3 and 4 for $v^+=0$ and $v^+=1$, respectively, some differences are worth noting. The most significant difference between rotational line intensities for the $v^+=0$ and the $v^+=1$ bands is that the negative ΔN lines, such as the N and O branch lines, are not seen in the $v^+=1$ band. This is not surprising if the mechanism for the added intensity is field-induced (or forced) rotational autoionization from lower principal quantum number Rydberg states.[38] Such states at energies above the $v^+=0$ limit can decay by other processes, such as vibrational autoionization, and are thus not long enough lived to be ionized by the pulsed field. There are other less significant differences in rotational line intensities, such as the difference in the relative strengths of the Q branch and $R(1)$ line in the two bands. However, based on peak areas, the Q branch is only 25% more intense in the $v^+=1$ spectrum. Similarly, the relative importance of the $T(0)$ and $S(1)$ lines reverses in the two bands. In both cases, however, they have roughly equal intensities, so this is not a major difference.

Figure 5(a) shows the measured and Fig. 5(b) shows the calculated PFI-ZEKE photoelectron spectra for single-photon ionization of rotationally cold N_2 ($X\,^1\Sigma_g^+$, $v''=0$) molecules by coherent XUV radiation leading to the $v^+=0$ level of N_2^+ ($X\,^2\Sigma_g^+$). Again, the calculated spectrum assumes a temperature of 8 K and a photoelectron energy of 50 meV and is convoluted with a Gaussian detection function with a FWHM of 2.7 cm^{-1}. Nuclear spin statistics are also taken into account in determining the populations of the rotational levels of N_2. The agreement between the calculated and measured spectra is excellent except for the O branches. It is again apparent that the abnormal intensities of these O branches with negative ΔN ($\Delta N=-2$) seen in the measured spectrum must arise from rotational autoionization.[15] Note that no $\Delta N=odd$ (N, P, R, or T branch) transitions occur in single-photon ionization of the $3\sigma_g$ orbital of the $X\,^1\Sigma_g^+$ ground state of N_2 in both the measured and calculated spectra. However, these $\Delta N=$odd branches are quite prominent in the photoelectron spectra of the 5σ orbital of the $X\,^1\Sigma^+$ state of CO (Figs. 3 and 4). According to the simple selection rule of $\Delta N+l=$odd,[23,24,34,35] these $\Delta N=$odd transitions must arise from even partial wave contributions to the photoelectron matrix elements. Since the $3\sigma_g$ orbital of N_2 has only even partial wave character, the photoelectron matrix element has odd partial wave components for single-photon ionization of this orbital and, hence, no $\Delta N=$odd transitions can

occur. The experimental results on jet cooled N_2 are in good agreement with earlier results of Merkt and Softley,[19] who recorded the PFI-ZEKE spectrum of room temperature N_2 and also found the intensity of the Q branch to be more than an order of magnitude stronger than the S branch.

Another significant difference between the calculated and measured PFI-ZEKE spectra of Figs. 3 and 5 concerns the intensities of the Q branches relative to other branches such as the $S(0)$ branch for N_2 and CO. The measured N_2 PFI-ZEKE spectrum shows a much larger Q to S branch intensity ratio than for CO. This is in contrast to the calculated spectra where these branch intensity ratios are comparable for N_2 and CO. Since the even partial wave content of the 5σ orbital of CO and the $3\sigma_g$ orbital of N_2 are quite similar, we do not expect the underlying photoionization dynamics of these orbitals to differ significantly. This is the case in the calculated spectra. To provide some further insight into the underlying photoelectron dynamics of this PFI process, we compare the angular momentum compositions of the photoelectron matrix element for both cases. The partial wave components of the photoelectron matrix element $r_{fi}^{l\lambda\mu}$ of Eq. (4) for single-photon ionization of CO, at a kinetic energy of 50 meV, are 0.0545, 0.7467, 0.3987, 0.050, and 0.0124 for $l=0$–4, respectively, in the $k\sigma$ channel, and 0.4580, 0.0721, 0.0820, and 0.0108 for $l=1$–4, respectively, in the $k\pi$ channel. The partial wave components for single-photon ionization of N_2 are 0.7991 and 0.1873 for $l=1$ and 3, respectively, in the $k\sigma_u$ channel and 0.5322 and 0.1285 for $l=1$ and 3, respectively, in the $k\pi_u$ channel. Clearly, odd ($l=1$ and 3) partial wave components are dominant in both cases, and these components are responsible for the most intense Q branches. The d wave of the $k\sigma$ channel for photoionization of CO is also important for the $\Delta N=$odd transitions due to the 24% p character of the 5σ orbital.

The reason for this disagreement between the *ab initio* intensities and the measured intensities for CO is not clear. This disagreement is especially intriguing since while the relative intensity of the Q branch is not well predicted, all other branches in the CO spectrum are reproduced very well by theory. As expected from previous PFI-ZEKE work, the intensities of the negative ΔN branches in the $v^+=0$ bands of N_2 and CO show the effect of field-induced rotational autoionization, which is absent in the CO $v^+=1$ spectrum.

One possible significant difference between CO and N_2 is the presence of strong autoionizing resonances at both the $v^+=0$ and $v^+=1$ thresholds in CO. We have investigated these resonances by looking at the total photoionization cross section for jet-cooled CO. For both $v^+=0$ and $v^+=1$, there are strong peaks exactly at threshold, with widths slightly larger than the PFI-ZEKE bands shown in Figs. 3 and 4. Existence of such resonances can affect the rotational line strengths through a complex resonance interaction,[18,21] but it is not clear how this could selectively reduce the Q branch lines (or selectively enhance the other branches). More theoretical studies are needed to understand the possible interactions with lower principal quantum number Rydberg states and the effects of these interactions on rotational line strengths.

ACKNOWLEDGMENTS

The experimental work done at Waterloo was supported by NSERC (Canada) and the Federal Networks of Centers of Excellence program, administered by NSERC. W. K. wishes to thank NSERC for a graduate scholarship. Work at the California Institute of Technology was supported by grants from the National Science Foundation, Air Force Office of Scientific Research, and the Office of Health and Environmental Research of the U. S. Department of Energy. We also acknowledge use of the resources of the Jet Propulsion Laboratory/California Institute of Technology CRAY Y-MP2E/116 supercomputer.

[1] K. Müller-Dethlefs and E. W. Schlag, Annu. Rev. Phys. Chem. **42**, 109 (1991).
[2] G. Reiser, W. Habenicht, K. Müller-Dethlefs, and E. W. Schlag, Chem. Phys. Lett. **152**, 119 (1988).
[3] R. G. Tonkyn, J. W. Winniczek, and M. G. White, Chem. Phys. Lett. **164**, 137 (1989).
[4] R. G. Tonkyn, R. Wiedmann, E. R. Grant, and M. G. White, J. Chem. Phys. **95**, 7033 (1991).
[5] K. S. Haber, Y. Jiang, G. P. Bryant, E. R. Grant, and H. Lefebvre-Brion, Phys. Rev. A **44**, 5331 (1991).
[6] G. Reiser and K. Müller-Dethlefs, J. Phys. Chem. **96**, 9 (1992).
[7] M. Braunstein, V. McKoy, S. N. Dixit, R. G. Tonkyn, and M. G. White, J. Chem. Phys. **93**, 5345 (1990).
[8] R. T. Wiedmann, R. G. Tonkyn, M. G. White, K. Wang, and V. McKoy, J. Chem. Phys. **97**, 768 (1992).
[9] H. Rudolph, V. McKoy, and S. N. Dixit, J. Chem. Phys. **90**, 2570 (1989).
[10] K. Wang and V. McKoy, J. Chem. Phys. **95**, 8718 (1991).
[11] M.-T. Lee, K. Wang, V. McKoy, R. G. Tonkyn, R. T. Wiedmann, E. R. Grant, and M. G. White, J. Chem. Phys. **96**, 7848 (1992).
[12] S. T. Pratt, J. Chem. Phys. (to be published).
[13] W. A. Chupka, J. Chem. Phys. **98**, 4520 (1993)
[14] R. T. Wiedmann and M. G. White, Proc. SPIE **1638**, 273 (1992).
[15] R. T. Wiedmann, R. G. Tonkyn, E. R. Grant, and M. G. White, J. Chem. Phys. **95**, 746 (1991).
[16] R. G. Tonkyn, R. T. Wiedmann, and M. G. White, J. Chem. Phys. **96**, 3696 (1992).
[17] W. Kong, D. Rodgers, and J. W. Hepburn, Chem. Phys. Lett. **203**, 497 (1993).
[18] F. Merkt and T. P. Softley, J. Chem. Phys. **96**, 4149 (1992).
[19] F. Merkt and T. P. Softley, Phys. Rev. A **46**, 302 (1992).
[20] W. Kong, D. Rodgers, and J. W. Hepburn, *Proceedings of the 10th International Conference on Vacuum Ultraviolet Physics* (1992).
[21] W. Kong, D. Rodgers, and J. W. Hepburn, J. Chem. Phys. (submitted).
[22] W. Kong, D. Rodgers, and J. W. Hepburn (unpublished).
[23] S. N. Dixit and V. McKoy, Chem. Phys. Lett. **128**, 49 (1986).
[24] K. Wang and V. McKoy, J. Chem. Phys. **95**, 4977 (1991).
[25] A. R. Edmonds, *Angular Momentum in Quantum Mechanics* (Princeton University, Princeton, NJ, 1974).
[26] T. H. Dunning, Jr., J. Chem. Phys. **53**, 2823 (1970).
[27] R. B. Singh and D. K. Rai, J. Mol. Spectrosc. **19**, 424 (1966).
[28] K. P. Huber and G. Herzberg, *Molecular Spectra and Molecular Structure. IV. Constants of Diatomic Molecules* (Van Nostrand, New York, 1979).
[29] I. Tobias, R. J. Fallon, and J. T. Vanderslice, J. Chem. Phys. **33**, 1638 (1960).
[30] R. R. Lucchese, G. Raseev, and V. McKoy, Phys. Rev. A **25**, 2572 (1982).
[31] R. R. Lucchese and V. McKoy, Phys. Rev. A **28**, 1382 (1983).
[32] R. L. Kelly, J. Phys. Chem. Ref. Data **16**, 1351 (1987).
[33] K.-P. Huber and F. Rostas (private communication of unpublished results).

[34] J. Xie and R. N. Zare, J. Chem. Phys. **93**, 3033 (1990).
[35] G. Raseev and N. Cherepkov, Phys. Rev. A **42**, 3948 (1990).
[36] M. Sander, L. A. Chewter, K. Müller-Dethlefs, and E. W. Schlag, Phys. Rev. A **36**, 4543 (1987).
[37] M. Takahashi, H. Ozeki, and K. Kimura, Chem. Phys. Lett. **181**, 255 (1991).
[38] F. Merkt, H. H. Fielding, and T. P. Softley, Chem. Phys. Lett. **202**, 153 (1993).